IJECBE (2024), **2**, **3**, 272–283
Received (7 July 2024) / Revised (5 July 2024)
Accepted (5 July 2024) / Published (30 September 2024)
https://doi.org/10.62146/ijecbe.v2i3.76
https://ijecbe.ui.ac.id
ISSN 3026-5258

International Journal of Electrical, Computer and Biomedical Engineering

RESEARCH ARTICLE

Optimizing Charge and Discharge of Lithium-Ion Batteries by Deploying PID Controller with Coupled Electro-Thermal-Aging Dynamic

Iwan Bahyudin Akbar, Ariono Verdianto, and Chairul Hudaya*

Department of Electrical Engineering, Faculty of Engineering, Universitas Indonesia, Depok, Indonesia
*Corresponding author. Email: chairul.hudaya@ui.ac.id

Abstract

Lithium-ion batteries (LIBs) are extensively utilized in many applications, from power plant utilities to portable electronic devices. Nevertheless, the performance and longevity of the LIB are affected by the interconnected electro-thermal-aging (ETA) dynamics that occur during the repeated process of charging and discharging. This study presents a technique for managing the charging and discharging of LIBs by controlling the operational voltage, addressing this issue. The technique involves employing a proportional-integral-derivative (PID) controller, which involves interconnected ETA dynamics. The result of the suggested technique is confirmed by comparing experimental data obtained from a cylindrical 26650 lithium-iron phosphate (LFP). The PID controller optimizes the response time of charging and discharging through the voltage while affecting the lifetime of the cell. The results indicated that the implementation of the PID controller allows for a rapid and secure charging and discharging process for LIB, leading to improved cell health and a longer cell life expectancy by controlling a certain degree of parameter known as overshoot. This strategy has a potential to be implemented in the charging and discharging process that positively affects the LIBs performance.

Keywords: Lithium-ion Batteries, Electric Circuit Model, Electro-Thermal-Aging Dynamic, PID

1. Introduction

LIB cells are extensively employed as electric energy storage devices because of their features, including low self-discharge rate, no memory effect, higher energy density per weight and volume, consistent performance, and a longer cycle life in comparison to alternative secondary battery kinds [1]. They are used in many systems including

portable electronics, electric cars, renewable energy systems, marine current energy systems, stationary energy storage, *etc.* [2] [3] [4]. The performance of the battery cell is affected by its degradation at microscopic levels. Furthermore, the phenomenon of overcharging and over discharging battery cells not only results in irreversible damage to the cells, but also poses potential safety hazards [5] [6]. To ensure the safety and reliability of LIBs throughout their operation, the battery management system (BMS) plays an important role in this scheme. It oversees several aspects such as charge/discharge cycles, temperature, state-of-charge (SOC), status of health (SOH), and current/voltage information, all of which are crucial for the user [7]. Since the quantifiable parameters of a battery are terminal voltage, current, and surface temperature, an effective BMS design requires efficient status and parameter estimation algorithms, which necessitate accurate battery models [8] [9]. Therefore, battery modeling must account for changes in internal parameters.

One of the key factors affecting LIB performance is the electro-thermal aging dynamics that occur during charge and discharge cycles. These dynamics involve complex interactions between electrical, thermal, and aging processes within the battery cell. To obtain accurate SOC estimates, precise battery models are essential. There are several dynamic models for LIB, including electrochemical models, neural network (NN) models, electric circuit models (ECM), and others [10]. The electrochemical model is a direct model presenting the chemical and electrochemical as well as the mechanical and transport laws, applying high-order differential equations which can predict closely to the real characteristics of LIBs. However, this strategy is usually characterized by a very high computational cost. In fact, electrochemical models consist of high order differential equations, such as pseudo two-dimensional (P2D) models, which are not suitable for online applications [11] [12]. On the other hand, to achieve the optimal result in modeling, the NN requires a huge bundle of experimental data for its calculation. The system does not need understanding of the precise electrochemical process [13]. Alternatively, it undergoes a reiteration process using a learning algorithm until the estimation error falls below a specific threshold. However, a direct variable extraction approach is still required to accurately determine the variables of the first-order equivalent circuit model (ECM) [12]. In contrast, the ECMs are usually identified by a less significant variable in estimating the battery cell parameter that mentioned above and are frequently employed in online applications. In fact, these models utilized a linear system such as an equivalent circuit which represents the elemental aspect of LIBs [14]. Nevertheless, in the most case, these values lack a tangible explanation and can just offer a depiction of abstract physical properties. ECM models in several research have been calibrated using an appropriate optimization technique, as the actual lumped parameter values are rarely known beforehand.

The 2RC model is regarded as a prototypical ECM battery model due to its distinctive nature in comparison to other systems and its practical potential application in the engineering world. A model incorporating a second-order resistance-capacitance (RC) circuit network provides more accurate predictions for the behavior of some battery cells [15]. The equivalent circuit model reflects the fluctuating voltage properties of a battery by employing resistors, capacitors, constant voltage sources, and other cir-

cuit components to construct a circuit network. This model is a frequently employed concentrated variable framework for system modeling and real-time management [16] [17] It is distinguished by its simplicity, as it typically has a limited number of variables, which makes it easier to derive the state space equation.

In this study, we use the 2RC ECM model because it can improve efficiency and battery lifespan. It can be achieved by adjusting the voltages U_{p1} through the utilization of a proportional-integral-derivative (PID) controller. The design of the PID controller for a lithium-ion battery (LIB) utilizing the ETA model necessitates this adjustment to guarantee optimal charging and discharging of the battery, while concurrently minimizing the detrimental impact of battery ageing on the battery. Moreover, the dynamic model of the ETA is implemented in MATLAB/Simulink through a PID controller. The model is then validated to evaluate the efficacy of this methodology by comparing to experimental data obtained from the datasheet of A123-ANR26650M1A battery (26650 LFP cell). The result indicated that a significant improvement in term of the cells cycle life, reflecting the impact of this strategy in improving the charging and discharging process.

2. Battery Modeling and Variable Input

2.1 Equivalent Circuit Model

Figure 1 illustrates that U_{oc} (SOC) denotes the open circuit voltage, which is directly related to the SOC of the battery. The term "ohmic resistance" is used to refer to the internal resistance of the battery, which is denoted as R_0.

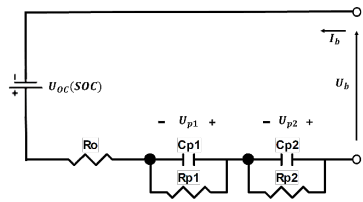

Figure 1. The proposed 2RC-ECM Model

$$SOC = \frac{1}{3600C_N} I_b \tag{1}$$

$$U_{p1} = \frac{1}{R_{p1}C_{p1}} U_{p1} + \frac{1}{C_{p1}} I_b \tag{2}$$

$$U_{p2} = \frac{1}{R_{p2}C_{p2}} U_{p2} + \frac{1}{C_{p2}} I_b \tag{3}$$

$$U_b = U_{oc}(SOC) + U_{p1} + U_{p2} + R_0 I_b \tag{4}$$

The presence of resistance in the circuit results in a reduction in voltage across the battery when current passes through it. The resistances R_{p1} and R_{p2} represent the resistances to polarization of the battery. The presence of these resistances results in a decrease in voltage across the battery due to the accumulation of polarization layers on the electrodes. C_{p1} and C_{p2} represent the capacitances associated with the polarization of the battery. The capacitances in question serve as energy storage devices, accumulating energy throughout the battery's charging process and subsequently releasing it during discharge. U_{p1} and U_{p2} represent the reduction in voltage across the polarization capacitances. The symbol I_b represents the electric current passing through the battery. The voltage measured at the battery terminals is represented by the symbol U_b.

2.2 Thermal Model

A thermal model is a mathematical representation of the thermal behavior of a system or piece of equipment. It is used to predict the temperature distribution and heat transfer within the system and to analyze the thermal performance of the system under different operating conditions.

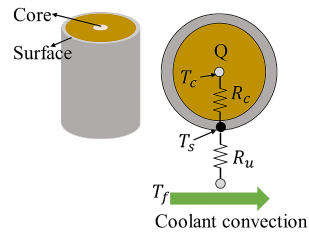

Figure 2. Thermal Model

Figure 2 presents a thermal model that represents the heat transfer dynamics of cylindrical battery cells. This model considers the impact of both the core temperature (T_c) and the surface temperature (T_s). T_c and T_s represent core temperature and surface temperature, respectively, while Tf denotes ambient temperature. T_c and T_s can be expressed in equations as follows [18]:

$$T_c = \frac{T_s - T_c}{R_c C_c} + \frac{Q(t)}{C_c} \tag{5}$$

$$T_s = \frac{T_f - T_s}{R_u C_s} - \frac{T_s - T_c}{R_c C_s} \tag{6}$$

R_c and R_u are radiation resistance and thermal resistance due to radiation, while C_c and C_s represent the heat capacitance of a battery. R_u is a function of the cooling convection flow rate, the rate of which can be adjusted to control the thermal behavior of the battery.

2.3 Aging Model

The aging model is a quantitative depiction of the deterioration processes that take place in lithium-ion batteries, which impact their functionality and longevity. The objective of the model is to forecast the SOH and lifespan of a battery by considering a number of parameters, including battery operation, battery consumption, and the materials employed. The battery capacity is a variable characteristic that diminishes over time as the battery is used. In accordance with the literature review, the formula for calculating C_{loss} is as follows [18]:

$$C_{loss} = M(I_c)exp\left[-\frac{E_a(I_c)}{R_g(273+T)}\right]Ah^z \tag{7}$$

$$A_{tol}(I_c, T_c) = \left[\frac{20}{M(I_c)exp\left(-\frac{E_a(I_c)}{R_g(273+T_c)}\right)}\right]^{1/z} \tag{8}$$

$$N(I_c, T_c) = \frac{3600A_{tol}(I_c, T_c)}{C_{bat}} \tag{9}$$

where C_{loss} is the percentage of capacity loss, $M(I_c)$ is pre-exponential factor as a function of C-rate, z is power-law factor, I_c is current of core, T_c is core temperature, A_{tol} is total discharge Ah throughput, N is number of cycles until end of life, C_{bat} is a cell's nominal capacity.

2.4 Electro-Thermal-Aging

The electro-thermal-aging dynamics in LIBs involve the combined aging process, which is influenced by both electrochemical and thermal variables. The number of charge cycles, voltage, and current, among other electrochemical parameters, can lead to the deterioration of internal components. Furthermore, thermal factors, such as the temperature of the battery, can also affect performance and lifespan. It has been demonstrated that elevated temperatures can accelerate electrochemical processes, resulting in battery deterioration. Furthermore, these reactions can subsequently elevate the battery temperature. It is therefore essential to gain a comprehensive understanding of these dynamics if we are to refine LIB solutions in order to effectively reduce the aging process and prolong the lifespan. The ETA approach integrates these factors to accurately reflect the performance of LIBs under diverse conditions. This is illustrated in Figure 3, where I_b (current) and T_f (temperature) are employed as inputs, while Ts, Tc (internal temperatures), and SOH are the resulting outputs.

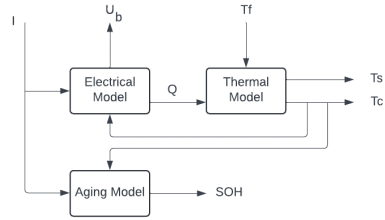

Figure 3. ETA Model

3. Research Methods

3.1 MATLAB/Simulink

Simulink is a block diagram environment used for multidomain simulation and model-based design, such as modeling dynamic systems using a graphical editor and customizable block libraries. Additionally, Simulink integrates with MATLAB, allowing MATLAB algorithms to be incorporated into models and facilitating further analysis of simulation results. This research utilizes MATLAB version R2021a. By creating Simulink blocks from the ETA model, a simulation diagram as shown in Figure 4 is obtained, comprising charge and discharge processes.

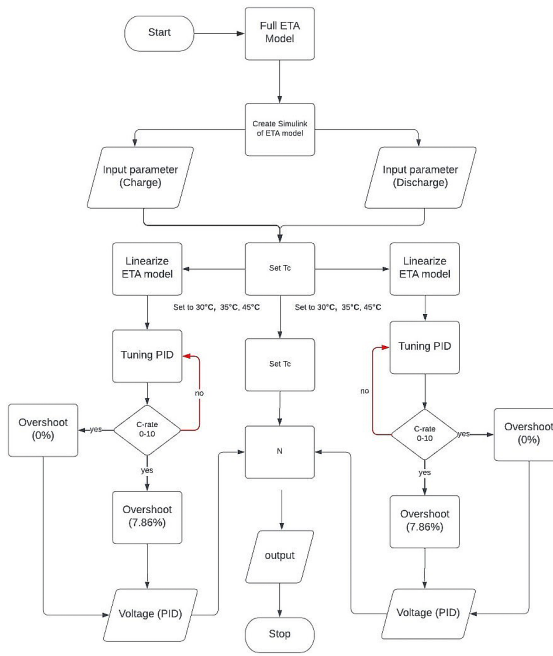

Figure 4. Flowchart diagram of the proposed method

Figure 4 shows a flowchart diagram derived from the full representation of the ETA model, which consists of several model subsystems. The charge and discharge blocks have the same full model, with the only difference being the input coefficients for each Simulink block. The Simulink block diagram above illustrates standard charging or discharging at a current of 3A for the A123-ANR26650M type.

3.2 PID Controller

PID is a feedback control loop commonly used in industry to regulate various process variables such as temperature, pressure, and flow. This controller operates by calculating the error in the system, which is the difference between the desired setpoint and the actual value of the process variable, and then adjusting based on three main components: proportional, integral, and derivative.

The proportional component reacts to the current error by adjusting the output directly. The correction provided is proportional to the magnitude of the error, resulting in a quick response to changes in the process variable. The integral component works by accumulating past errors and making adjustments to address persistent errors, helping achieve a stable condition without sustained errors. The derivative component focuses on the rate of change of the error and provides adjustments based on how quickly the error is changing. This helps dampen sudden changes in the process variable and enhances system stability.

In this study, we control the voltages U_{p1c} (charge) of LIBs using the ETA model, including the PID control process on ETA. In detail, the selection of PID parameters utilises the reference voltage value U_{p1c}, which is the polarised battery voltage. Subsequently, the control values the proportional gain (K_p), integral gain (K_i), and derivative gain (K_d) are determined, which serve as the inputs for the ETA model. The aforementioned parameters are then tuned using SIMULINK in order to produce a voltage that is controlled by the PID.

4. Results and Discussion

The relationship between SOC and parameters for charging and discharging LIBs can be observed in Figure 5. The charging and discharging coefficients for LIBs are found in the experimental data.

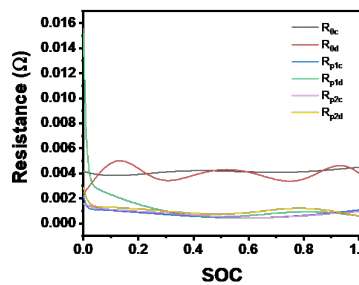

Figure 5. The relationship between Ohmic resistance (R_{0c}, R_{0d}, R_{p1c}, R_{p2c}, R_{p1d}, R_{p2d}) *vs.* SOC.

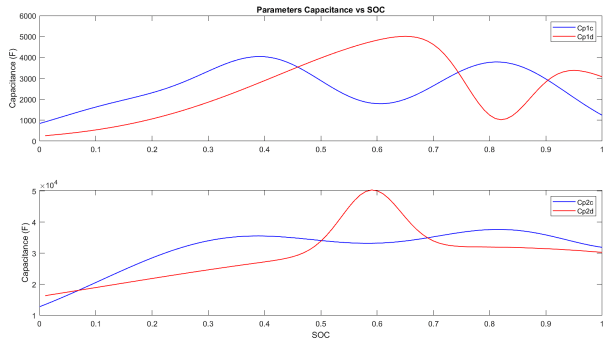

Figure 6. The parameter of capacitance (C_{p1c}, C_{p2c}, C_{p1d}, C_{p2d}) vs SOC

R_{0c} represents the parameter of Ohmic resistance during charging, while R_{0d} represents the parameter of Ohmic resistance during discharge. During the discharging process of LIBs, R_{0d} tends to increase. The relationship between SOC and resistance parameters during both charging and discharging of LIB can be understood from Figure 5, R_{p1c} and R_{p2c} represent the charging resistances of LIB, while R_{p1d} and R_{p2d} represent the discharging resistances. C_{p1c} and C_{p2c} denote the charging capacities of LIB, whereas C_{p1d} and C_{p2d} denote the discharging capacities. According to Figure 5, the values of R_{p1c} and R_{p2c} decrease significantly. This demonstrates that during both the charging and discharging processes of the battery, the power dissipation decreases when the battery is fully charged.

Based on Figure 6, the parameter of capacitance (C_{p1c}, C_{p2c}, C_{p1d}, C_{p2d}) vs. SOC, these curves show how the capacitance of a system changes during charging and discharging. The capacitance C_{p1c} and C_{p1d} showed fluctuate graph during charging, the C_{p1c} increase from SOC 0 to SOC = 0.4 and decrease until SOC = 0.6 but C_{p1d} increase until SOC around 0.7 this happened because of the coefficient of parameters. C_{p2c} and C_{p2d} or double layer polarisation when SOC around 0.6 for C_{p2d} the capacitance reached around 50000(F).

During the charging or discharging of LIB, capacitance and resistance vary, which can affect the performance and efficiency of the LIB. Therefore, an optimal control model is needed to maintain the performance and efficiency of the battery. The simulation results of U_{oc} (SOC) and SOC against temperature differences can be observed in Figure 7, where X, Y, Z represent temperature, SOC, and voltage U_{oc} (SOC).

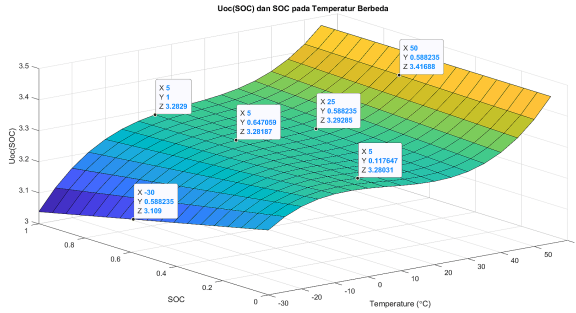

Figure 7. U_{oc} (SOC) over the SOC range and temperatures of -30 °C to 55 °C

The relationship of U_{oc} (SOC) voltage to SOC and temperature difference when SOC is constant at 3 setpoints of 0.588235 viz: when (X=-30, Y=0.588235, Z=3.109), (X=25, Y=0.588235, Z=3.29285) and (X=50, Y=0.588235, Z=3.41688). The value of Uoc(SOC) increases with temperature. However, when the temperature is constant in Figure 4.4 with 3 setpoints, namely a temperature of 50°C, obtained values at setpoints (X=5, Y=1, Z=3.2829), (X=5, Y=0.647059, Z=3.28187) and (X=5, Y=0.117647, Z=3.28031).

4.1 Voltage simulation employing PID controller

When tuning the voltage U_{p1c} using a PID controller, the goal is to find optimal values for the K_p, K_i, and K_d. This process is used to minimize the error between the setpoint and the actual variable. In this study, based on simulation, the value of U_{p1c} is 0.0015 under conditions where the C-rate is 2 and SOC is 0.7.

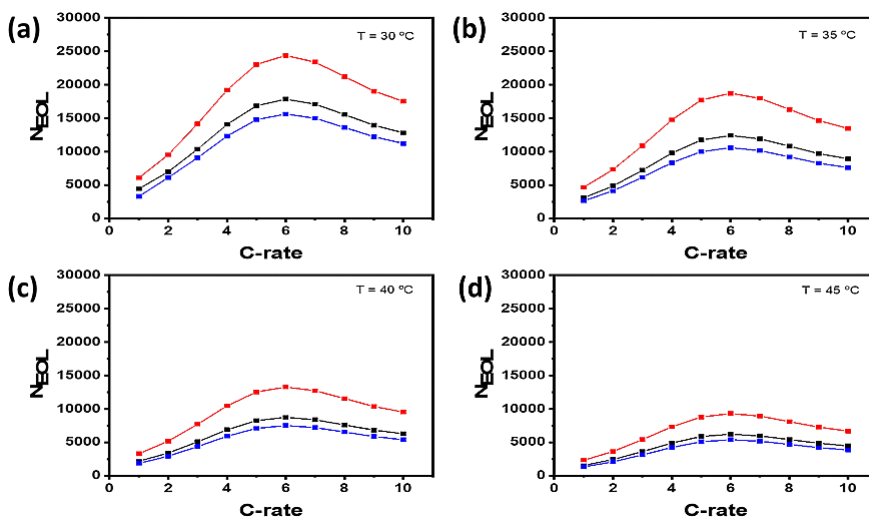

Figure 8. The parameter of capacitance (C_{p1c}, C_{p2c}, C_{p1d}, C_{p2d}) vs SOC

Figure 8. Battery cycle life vs C-rate at different temperature (°C), a) T=30 °C, b) =35 °C, c) =40 °C and d) =45 °C. The black color: reference; blue: PID controller with overshoot; and red: PID controller with non-overshoot.

In an end-of-life (EOL) cycle with a C-rate range of 0 to 10 at various temperatures between 30°C and 45°C. In Figure 8, the PID controller with overshoot shows the tuned voltage U_{p1c} gives a rise time of 1.15 seconds and a settling time of 4.08 seconds and the overshoot obtained is 7.86%. The reference values under conditions where C-rate = 2, SOC = 0.7 and temperature 30 °C or the LIB are as follows: A_{tol} = 9771 with a cycle number (N) = 4442. Temperature is a crucial factor that greatly affects the performance of lithium-ion batteries and restricts their practical applications. This result has been confirmed from the previous study in the literature [19].

Table 1. The reference of C-rate, A_{tol} and N based on the ETA Model when T = 30°C from the datasheet of LFP [18].

SOC	C-rate	A_{tol}	N
0.7	2	9771	4442

Table 2. C-rate, A_{tol} and N based on the ETA Model when T= 30 °C

		Overshoot (7.86%) Rise time (1.15 seconds)		Overshoot (0%) Rise time (8.25 seconds)	
SOC	C-rate	A_{tol}-PID	N_PID	A_{tol}-PID	N-PID
0.7	2	13445	6111	20968	9531

After PID control tuning, the values obtained are A_{tol}–PID = 13445 and N–PID = 6111. These values are lower because the PID tuning resulted in faster rise time 1.15 seconds and settling time 4.08 seconds compared to the initial conditions. However, in the case where there is no overshoot (0% OS), with rise time = 8.25 seconds and settling time = 14.1 seconds, the values obtained are A_{tol}–PID (0% OS) = 20968 and N–PID (0% Overshoot) = 9531.

5. Conclusion

This study presents a new approach to optimize the charging and discharging of LIBs by considering combined electro-thermal-aging dynamics. The proposed PID controller demonstrates effective performance in regulating charging conditions, battery voltage, and temperature, thereby minimizing aging impact. The PID controller employed for controlling U_{p1c} shows faster response time by 1.15 seconds in PID rise time or 1.35 seconds faster than before tuning and settling time of 4.08 seconds with overshoot 7.86%, N_{PID} of 6111 were obtained with an *overshoot* of 7.86%. In addition, if the overshoot PID of 0%, the rise time of 8.25 seconds and the settling time of 14.1 sec, the cycle number (N) without overshoot would be 9531 cycles. This means that with less overshoot in PID tuning, the cycle number will increase, but if the faster response time results in a decreased cycle number (N), which affects the batteries SOH, leading to deterioration of the batteries performance.

Acknowledgement

This work was supported by Competitive Research Grant funded by Ministry of Education, Culture, Research and Technology, Republic of Indonesia under the Applied Research Scheme with main contract No. 051/E5/PG.02.00.PL/2024 and sub-contract No. NKB-929/UN2.RST/HKP.05.00/2024.

References

[1] M. H. Hossain et al. "Advances of lithium-ion batteries anode materials—A review". In: *Chemical Engineering Journal Advances* 16 (Nov. 15, 2023), p. 100569.

[2] M. Şen, M. Özcan, and Y. R. Eker. "A review on the lithium-ion battery problems used in electric vehicles". In: *Next Sustainability* 3 (Jan. 1, 2024), p. 100036.

[3] M. Amir et al. "Energy storage technologies: An integrated survey of developments, global economical/environmental effects, optimal scheduling model, and sustainable adaption policies". In: *Journal of Energy Storage* 72 (Nov. 30, 2023), p. 108694.

[4] J. Mitali, S. Dhinakaran, and A. A. Mohamad. "Energy storage systems: a review". In: *Energy Storage and Saving* 1.3 (Sept. 1, 2022), pp. 166–216.

[5] Y. Yang et al. "Towards a safer lithium-ion batteries: A critical review on cause, characteristics, warning and disposal strategy for thermal runaway". In: *Advances in Applied Energy* 11 (Sept. 1, 2023), p. 100146.

[6] S. Rada et al. "Performance of the Recycled and Copper-Doped Materials from Spent Electrodes by XPS and Voltammetric Characteristics". In: *Journal of The Electrochemical Society* 167.9 (June 8, 2020), p. 090548.

[7] J. Tian, R. Xiong, and W. Shen. "State-of-Health Estimation Based on Differential Temperature for Lithium Ion Batteries". In: *IEEE Transactions on Power Electronics* PP (Mar. 5, 2020), pp. 1–1.

[8] V. Sangwan et al. *Equivalent circuit model parameters estimation of Li-ion battery: C-rate, SOC and Temperature effects*. 2016.

[9] Q. Yu et al. "Lithium-Ion Battery Parameters and State-of-Charge Joint Estimation Based on H-Infinity and Unscented Kalman Filters". In: *IEEE Transactions on Vehicular Technology* PP (May 29, 2017), pp. 1–1.

[10] M. N. Amiri et al. "Lithium-ion battery digitalization: Combining physics-based models and machine learning". In: *Renewable and Sustainable Energy Reviews* 200 (Aug. 1, 2024), p. 114577.

[11] K. Liu et al. "Electrochemical modeling and parameterization towards control-oriented management of lithium-ion batteries". In: *Control Engineering Practice* 124 (Apr. 3, 2022).

[12] N. A. Chaturvedi et al. "Algorithms for Advanced Battery-Management Systems". In: *IEEE Control Systems Magazine* 30.3 (2010), pp. 49–68.

[13] A. Jokar et al. "Review of simplified Pseudo-two-Dimensional models of lithium-ion batteries". In: *Journal of Power Sources* 327 (Sept. 30, 2016), pp. 44–55.

[14] R. Zhang et al. "Study on the Characteristics of a High Capacity Nickel Manganese Cobalt Oxide (NMC) Lithium-Ion Battery—An Experimental Investigation". In: *Energies* 11.9 (2018). DOI: 10.3390/en11092275.

[15] S. Leonori et al. "A Physically Inspired Equivalent Neural Network Circuit Model for SoC Estimation of Electrochemical Cells". In: *Energies* 14.21 (2021). DOI: 10.3390/en14217386.

[16] M.-K. Tran et al. "Comparative Study of Equivalent Circuit Models Performance in Four Common Lithium-Ion Batteries: LFP, NMC, LMO, NCA". In: *Batteries* 7.3 (2021). DOI: 10.3390/batteries7030051.

[17] X. Hu, S. Li, and H. Peng. "A comparative study of equivalent circuit models for Li-ion batteries". In: *Journal of Power Sources* 198 (Jan. 15, 2012), pp. 359–367.

[18] H. E. Perez et al. "Optimal Charging of Li-Ion Batteries With Coupled Electro-Thermal-Aging Dynamics". In: *IEEE Transactions on Vehicular Technology* 66.9 (2017), pp. 7761–7770.

[19] S. Ma et al. "Temperature effect and thermal impact in lithium-ion batteries: A review". In: *Progress in Natural Science: Materials International* 28.6 (Dec. 1, 2018), pp. 653–666.